

RESEARCH ARTICLE




Open Access

Open Data

Open Code

# Modelling the impact of the macroalgae *Asparagopsis taxiformis* on rumen microbial fermentation and methane production

Rafael Muñoz-Tamayo<sup>1\*</sup> , Juana C. Chagas<sup>2</sup>, Mohammad Ramin<sup>2</sup>, and Sophie J. Krizsan<sup>2</sup>

\*Correspondence:  
Rafael.munoz-tamayo@inrae.fr

<sup>1</sup> Université Paris-Saclay, INRAE, AgroParisTech, UMR Modélisation Systémique Appliquée aux Ruminants, 75005, Paris, France.

<sup>2</sup> Department of Agricultural Research for Northern Sweden, Swedish University of Agricultural Sciences (SLU), Skogsmarksgränd, 90183 Umeå, Sweden.

## Abstract

**Background:** The red macroalgae *Asparagopsis taxiformis* is a potent natural supplement for reducing methane production from cattle. *A. taxiformis* contains several anti-methanogenic compounds including bromoform that inhibits directly methanogenesis. The positive and adverse effects of *A. taxiformis* on the rumen microbiota are dose-dependent and operate in a dynamic fashion. It is therefore key to characterize the dynamic response of the rumen microbial fermentation for identifying optimal conditions on the use of *A. taxiformis* as a dietary supplement for methane mitigation. Accordingly, the objective of this work was to model the effect of *A. taxiformis* supplementation on the rumen microbial fermentation under *in vitro* conditions. We adapted a published mathematical model of rumen microbial fermentation to account for *A. taxiformis* supplementation. We modelled the impact of *A. taxiformis* on the fermentation and methane production by two mechanisms, namely (i) direct inhibition of the growth rate of methanogens by bromoform and (ii) hydrogen control on sugars utilization and on the flux allocation towards volatile fatty acids production. We calibrated our model using a multi-experiment estimation approach that integrated experimental data with six macroalgae supplementation levels from a published *in vitro* study assessing the dose-response impact of *A. taxiformis* on rumen fermentation.

**Results:** our model captured satisfactorily the effect of *A. taxiformis* on the dynamic profile of rumen microbial fermentation for the six supplementation levels of *A. taxiformis* with an average determination coefficient of 0.88 and an average coefficient of variation of the root mean squared error of 15.2% for acetate, butyrate, propionate, ammonia and methane.

**Conclusions:** our results indicated the potential of our model as prediction tool for assessing the impact of additives such as seaweeds on the rumen microbial fermentation and methane production *in vitro*. Additional dynamic data on hydrogen and bromoform are required to validate our model structure and look for model structure improvements. We expect this model development can be useful to help the design of sustainable nutritional strategies promoting healthy rumen function and low environmental footprint.

**Keywords:** greenhouse gas mitigation, hydrogen control, methane inhibitors, methane mitigation, red seaweed, rumen fermentation, rumen microbiota, rumen model.

## 1 1. Background

2 Some macroalgae (seaweeds) have the potential to be used as natural supplement for  
3 reducing methane (CH<sub>4</sub>) production from cattle (Wang *et al.*, 2008; Dubois *et al.*, 2013; Maia  
4 *et al.*, 2016). This anti-methanogenic activity adds value to the nutritional and healthy  
5 promoting properties of macroalgae in livestock diets (Evans and Critchley, 2014; Makkar *et al.*,  
6 2016). The species of the red macroalgae *Asparagopsis* have proven a strong anti-  
7 methanogenic effect both *in vitro* (Machado *et al.*, 2014) and *in vivo* (Roque *et al.*, 2019). In  
8 particular, *Asparagopsis taxiformis* appears as the most potent species for methane mitigation  
9 with studies reporting a reduction in enteric methane up to 80% in sheep (Li *et al.*, 2016) and  
10 up to 80% and 98% in beef cattle (Kinley *et al.*, 2020; Roque *et al.*, 2020). The anti-  
11 methanogenic power of *A. taxiformis* results from the action of its multiple secondary  
12 metabolites with antimicrobial activities, being bromoform the most abundant anti-  
13 methanogenic compound (Machado *et al.*, 2016b). It should be said, however, that despite  
14 the promising anti-methanogenic capacity of bromoform, the feasibility of supplying  
15 bromoform-containing macroalgae requires a global assessment to insure safety of feeding  
16 and low environmental footprint from the algae processing, since bromoform can be toxic to  
17 the environment and can impair human health (Beauchemin *et al.*, 2020).

18 Bromoform is released from specialised gland cells of the macroalga (Paul *et al.*, 2006) in to  
19 the culture medium. The mode of action of the anti-methanogenic activity of bromoform is  
20 similar to that described for bromochloromethane (Denman *et al.*, 2007), following the  
21 mechanism suggested for halogenated hydrocarbons (Wood *et al.*, 1968; Czerkawski and  
22 Breckenridge, 1975). Accordingly, bromoform inhibits the cobamid dependent methyl-  
23 transfer reactions that lead to methane formation. In addition to the direct effect on the  
24 methanogenesis, the antimicrobial activity of *A. taxiformis* impacts the fermentation profile  
25 (*e.g.*, acetate:propionate ratio) and the structure of the rumen microbiota (*e.g.*, the relative  
26 abundance of methanogens) (Machado *et al.*, 2018; Roque *et al.*, 2019). Fermentation  
27 changes may have detrimental effects on animal health and productivity (Chalupa, 1977; Li *et al.*,  
28 2016). Detrimental effects might include deterioration of the ruminal mucosa and the  
29 transfer of bromoform to tissues, blood and milk. Previous studies have not detected  
30 bromoform in animal tissues (Li *et al.*, 2016; Kinley *et al.*, 2020; Roque *et al.*, 2020). The  
31 positive and adverse effects of *A. taxiformis* on the rumen microbiota are dose-dependent  
32 (Machado *et al.*, 2016a) and operate in a dynamic fashion. It is therefore key to characterize  
33 the dynamic response of the rumen microbial fermentation for identifying optimal conditions  
34 on the use of the *A. taxiformis* as a dietary supplement for methane mitigation. The  
35 development of dynamic mathematical models provides valuable tools for the assessment of  
36 feeding and mitigation strategies (Ellis *et al.*, 2012) including developments in the  
37 manipulation of the flows of hydrogen to control rumen fermentation (Ungerfeld, 2020).  
38 Progress on rumen modelling including a better representation of the rumen microbiota and  
39 the representation of additives on the fermentation is central for the deployment of predictive  
40 tools that can guide microbial manipulation strategies for sustainable livestock production  
41 (Huws *et al.*, 2018). Accordingly, the objective of this work was to model the effect of *A.*  
42 *taxiformis* supplementation on the dynamics of rumen microbial fermentation under *in vitro*  
43 conditions. We adapted a published rumen fermentation model (Muñoz-Tamayo *et al.*, 2016)  
44 to account for the impact of *A. taxiformis* on rumen fermentation and methane production  
45 evaluated *in vitro* at six supplementation levels (Chagas *et al.*, 2019).

## 46 2. Methods

### 47 2.1. Experimental data

48 Model calibration was performed using experimental data from an *in vitro* batch study  
49 assessing the dose-response impact of *A. taxiformis* on fermentation and methane production  
50 (Chagas *et al.*, 2019). In such a study, *A. taxiformis* with 6.84 mg/g DM bromoform  
51 concentration was supplemented at six treatment levels (0, 0.06, 0.13, 0.25, 0.5, and 1.0 % of  
52 diet organic matter; OM). All experimental treatments were composed of a control diet  
53 consisted of timothy grass (*Phleum pratense*), rolled barley (*Hordeum vulgare*), and rapeseed  
54 (*Brassica napus*) meal in a ratio of 545:363:92 g/kg diet dry matter (DM) presenting chemical  
55 composition as 944 g/kg OM, 160 g/kg crude protein (CP) and 387 g/kg neutral detergent fiber  
56 (NDF). Prior to each *in vitro* incubation, dried individual ingredients milled at 1 mm were  
57 weighted into serum bottles totalizing 1000 mg substrate on DM basis. The incubation was  
58 carried out with rumen inoculum from two lactating Swedish Red cows cannulated in the  
59 rumen, fed ad libitum on a diet of 600 g/kg grass silage and 400 g/kg concentrate on DM basis.  
60 Diet samples were incubated for 48 h in 60 ml of buffered rumen fluid (rumen fluid:buffer  
61 ratio of 1:4 by volume) as described by Chagas *et al.* (2019). The *in vitro* batch fermentation  
62 was run in a fully automated system that allows continuous recording of gas production  
63 (Ramin and Huhtanen, 2012).

64 Methane production, acetate, butyrate, propionate, and ammonia were measured  
65 throughout the incubation period. Methane was measured at 0, 2, 4, 8, 24, 36 and 48 h  
66 according to (Ramin and Huhtanen, 2012). Gas production was measured using a fully  
67 automated system (Gas Production Recorder, GPR-2, Version 1.0 2015, Wageningen UR), with  
68 readings made every 12 min and corrected to the normal air pressure (101.3 kPa). Methane  
69 concentration was determined with a Varian Star 3400 CX gas chromatograph (Varian  
70 Analytical Instruments, Walnut Creek, CA, USA) equipped with a thermal conductivity  
71 detector. The volatile fatty acids (VFAs) were measured at 0, 8, 24 and 48 h and determined  
72 using a Waters Alliance 2795 UPLC system as described by (Puhakka *et al.*, 2016). Ammonia  
73 was measured at 0 and 24h and analysed with a continuous flow analyzer (AutoAnalyzer 3 HR,  
74 SEAL Analytical Ltd., Southampton, UK) and according to the method provided by SEAL  
75 Analytical (Method no. G-102-93 multitest MT7). For model calibration, we only considered  
76 data until 24h, since microbial fermentation stopped around this time.

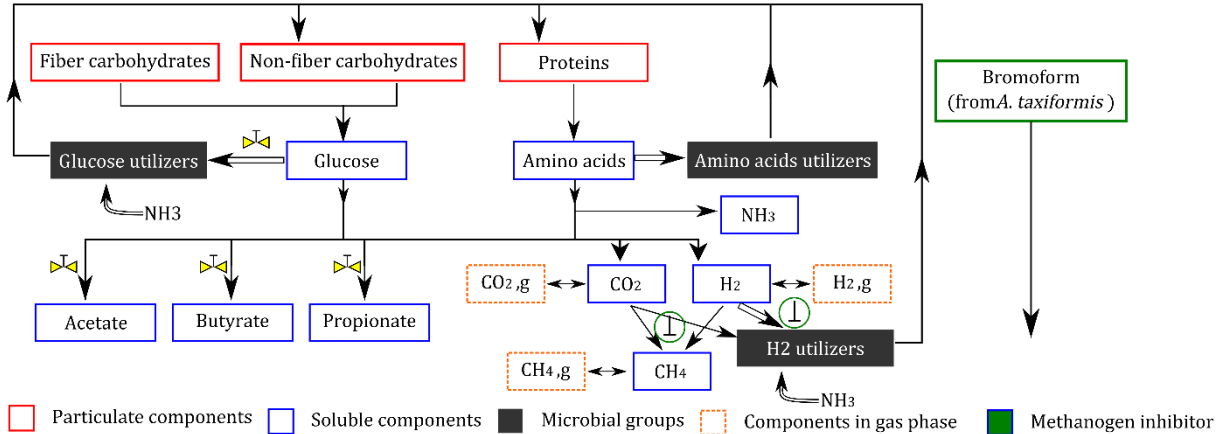
77

### 78 2.2. Mathematical modelling

79 We adapted the mathematical model of *in vitro* rumen fermentation developed by (Muñoz-  
80 Tamayo *et al.*, 2016) to account for the effect of *A. taxiformis* on the fermentation. This model  
81 represents the rumen microbiota by three microbial functional groups (sugar utilisers, amino  
82 acid utilisers and methanogens). Hexose monomers are represented by glucose and amino  
83 acids are represented by an average amino acid. The model is an aggregated representation  
84 of the anaerobic digestion process that comprises the hydrolysis of cell wall carbohydrates  
85 (NDF - Neutral Detergent Fiber), non-fiber carbohydrates (NSC - Non Structural  
86 Carbohydrates) and proteins, the fermentation of soluble monomers producing the VFAs  
87 acetate, butyrate, propionate, and the hydrogenotrophic methanogenesis. The original  
88 model was calibrated using *in vitro* experimental data from (Serment *et al.*, 2016). Figure 1

89 displays a schematic representation of the rumen fermentation model indicating the effect of  
 90 *A. taxiformis* on the fermentation. We assumed that microbial cells are formed by proteins  
 91 and non-fiber carbohydrates and that dead microbial cells are recycled as carbon sources in  
 92 the fermentation.

93



95 **Figure 1.** Representation of the rumen fermentation model (adapted from (Muñoz-Tamayo *et al.*, 2016)). Hydrolysis of carbohydrates (fiber and non-fiber) and proteins releases  
 96 respectively sugars and amino acids soluble monomers which are further utilized by the  
 97 microbiota. The utilization of substrate is directed to product formation (single arrows) and  
 98 microbial growth (double arrows). Each substrate is utilized by a single microbial functional  
 99 group. The bromoform contained in *A. taxiformis* produces a direct inhibition of the growth  
 100 rate of methanogens that results in a reduction of methane production and in an  
 101 accumulation of hydrogen. The symbol  $\textcircled{\perp}$  indicates the direct effect of the bromoform on the  
 102 methanogenesis. Hydrogen exerts control on sugars utilization and on the flux allocation  
 103 towards volatile fatty acids production. The symbol  $\textcircled{\triangleright}$  indicates the hydrogen control effect  
 104 on the rumen fermentation.

106

107 The model is derived from mass balance equations of a closed system under the assumption  
 108 that the protocol of gas sampling does not affect substantially the dynamics of methane and  
 109 fermentation dynamics. Our model is described in compact way as follows

110 
$$\frac{d\xi}{dt} = \mathbf{S} \cdot \boldsymbol{\rho}(\xi, \mathbf{p}) - \mathbf{g}(\xi, \mathbf{p}) \quad (1)$$

111 Where  $\xi$  is the vector of state variables (metabolites),  $\boldsymbol{\rho}(\cdot)$  is a vector function with the kinetic  
 112 rates of hydrolysis and substrate (sugars, amino acids, hydrogen) utilization. Hydrolysis rates  
 113 are described by first-order kinetics. Substrate utilization rates are described by the Monod  
 114 kinetics.  $\mathbf{S}$  is the stoichiometry matrix containing the yield factors ( $Y_{i,j}$ ) of each metabolite ( $i$ )  
 115 for each reaction ( $j$ ),  $\mathbf{g}(\cdot)$  is a vector function with the equations representing transport  
 116 phenomena (liquid–gas transfer), and  $\mathbf{p}$  is the vector of the model parameters. The original  
 117 model has 18 state variables (compartments in Figure. 1) and was implemented in Matlab (the  
 118 code is accessible at <https://doi.org/10.5281/zenodo.4047640>). An implementation in R  
 119 software is also available (Kettle *et al.*, 2018). In the present work, we incorporated an  
 120 additional state variable to represent the dynamics of bromoform concentration. The original  
 121 model was extended to account for the impact of *A. taxiformis* on the rumen fermentation.  
 122 While the original model predicts the pH, we set the pH value to 6.6.

123

124 The impact of *A. taxiformis* on the fermentation and methane production was ascribed to two  
125 mechanisms, namely the (i) direct inhibition of the growth rate of methanogens by  
126 bromoform and (ii) hydrogen control on sugars utilization and on the flux allocation towards  
127 volatile fatty acids production. These aspects are detailed below.

128

129 For the methanogenesis, the reaction rate of hydrogen utilization  $\rho_{H_2}$  (mol/(L h)) is given by

130

131 
$$\rho_{H_2} = I_{br} \cdot I_{IN} \cdot k_{m,H_2} \frac{s_{H_2}}{K_{s,H_2} + s_{H_2}} x_{H_2} \quad (2)$$

132

133 where  $s_{H_2}$  (mol/L) is the hydrogen concentration in liquid phase,  $x_{H_2}$  (mol/L) is the  
134 concentration of hydrogen-utilizing microbes (methanogens),  $k_{m,H_2}$  (mol/(mol h)) is the  
135 maximum specific utilization rate constant of hydrogen and  $K_{s,H_2}$  (mol/L) is the Monod affinity  
136 constant of hydrogen utilization, and  $I_{IN}$  is a nitrogen limitation factor. The kinetic rate is  
137 inhibited by the anti-methanogenic compounds of *A. taxiformis*. The factor  $I_{br}$  represents this  
138 inhibition as function of the bromoform concentration. We used the following sigmoid  
139 function to describe  $I_{br}$

140

141 
$$I_{br} = 1 - \frac{1}{1 + \exp(-p_1 \cdot (s_{br} + p_2))} \quad (3)$$

142

143 where  $s_{br}$  is the bromoform concentration (g/L) and  $p_1, p_2$  are the parameters of the sigmoid  
144 function. We included in our model the dynamics of bromoform using a first-order kinetics to  
145 take into account that the inhibition of *A. taxiformis* declines on time as a result of the  
146 consumption of anti-methanogenic compounds (Kinley *et al.*, 2016). The dynamics of  $s_{br}$  is

147

148 
$$\frac{ds_{br}}{dt} = -k_{br} \cdot s_{br} \quad (4)$$

149

150 where  $k_{br}$  (1/h) is the kinetic rate constant of bromoform utilization.

151

152 With regard to sugars utilization, we assumed that the effect of *A. taxiformis* is ascribed to  
153 hydrogen control due to accumulation of hydrogen resulting from the methanogenesis  
154 inhibition. Hydrogen level influences the fermentation pattern (Janssen, 2010). We used the  
155 structure proposed by (Mosey, 1983) to account for hydrogen control on sugar utilization and  
156 flux allocation. However, we used different parametric functions to those proposed by  
157 (Mosey, 1983). The functions proposed by (Mosey, 1983) did not provide satisfactory results.

158

159 In our model, the kinetic rate of sugar utilization is described by

160

161 
$$\rho_{su} = I_{H_2} \cdot I_{IN} \cdot k_{m,su} \frac{s_{su}}{K_{s,su} + s_{su}} x_{su} \quad (5)$$

162 where  $s_{su}$  (mol/L) is the concentration of sugars,  $x_{su}$  (mol/L), is the concentration of sugar  
163 utilisers microbes,  $k_{m,su}$  (mol/(mol h)) is the maximum specific utilization rate constant of  
164 sugars and  $K_{s,su}$  (mol/L) is the Monod affinity constant of sugars utilization.

165

166 The factor  $I_{H_2}$  describes the hydrogen inhibition:

167

$$168 \quad I_{H_2} = 1 - \frac{1}{1 + \exp(-p_3 \cdot (p_{H_2} + p_4))} \quad (6)$$

169 with  $p_{H_2}$  the hydrogen partial pressure ( $p_{H_2}$ ).

170

171 In our model, the rumen fermentation is represented by the macroscopic reactions in Table

172 1.

173

174 **Table 1.** Macroscopic reactions used in our model to representing rumen fermentation. For

175 the anabolic reactions of microbial formation, we assume that microbial biomass has the

176 molecular formula  $C_5H_7O_2N$ .

177

<i>Sugars (glucose) utilization</i>	
$C_6H_{12}O_6 + 2H_2O \rightarrow 2CH_3COOH + 2CO_2 + 4H_2$	R <sub>1</sub>
$3C_6H_{12}O_6 \rightarrow 2CH_3COOH + 4CH_3CH_2COOH + 2CO_2 + 2H_2O$	R <sub>2</sub>
$C_6H_{12}O_6 \rightarrow CH_3CH_2CH_2COOH + 2CO_2 + 2H_2$	R <sub>3</sub>
$5C_6H_{12}O_6 + 6NH_3 \rightarrow 6C_5H_7O_2N + 18H_2O$	R <sub>4</sub>
<i>Amino acid utilization</i>	
$C_5H_9.8O_{2.7}N_2 \rightarrow Y_{IN,aa}NH_3 + (1 - Y_{aa}) \cdot \sigma_{ac,aa} CH_3COOH + (1 - Y_{aa}) \cdot \sigma_{pr,aa} CH_3CH_2COOH + (1 - Y_{aa}) \cdot \sigma_{bu,aa} CH_3CH_2CH_2COOH + (1 - Y_{aa}) \cdot \sigma_{1C,aa} CO_2 + (1 - Y_{aa}) \cdot \sigma_{H_2,aa} H_2 + Y_{aa}C_5H_7O_2N$	R <sub>5</sub> *
<i>Hydrogen utilization</i>	
$4H_2 + 2CO_2 \rightarrow CH_4 + 2H_2O$	R <sub>6</sub>
$10H_2 + 5CO_2 + NH_3 \rightarrow C_5H_7O_2N + 8H_2O$	R <sub>7</sub>

178 \*R<sub>5</sub> is an overall reaction resulting from weighing the fermentation reactions of individual amino acids.

179

180 Table 1 shows that VFA production from glucose utilization occurs *via* reactions R<sub>1</sub>-R<sub>3</sub>. The

181 pattern of the fermentation is determined by the flux allocation of glucose utilization through

182 these three reactions. We denote  $\lambda_k$  as the molar fraction of the sugars utilized *via* reaction

183  $k$ . It follows that  $\lambda_1 + \lambda_2 + \lambda_3 = 1$ .

184 The fermentation pattern (represented in our model by the flux allocation parameters  $\lambda_k$ ) is

185 controlled by thermodynamic conditions and by electron-mediating cofactors such as

186 nicotinamide adenine dinucleotide (NAD) that drive anaerobic metabolism via the transfer of

187 electrons in metabolic redox reactions (Mosey, 1983; Hoelzle *et al.*, 2014; van Lingen *et al.*,

188 2019). In our model, the regulation exerted by the NADH/NAD<sup>+</sup> couple on the flux allocation

189 is incorporated *via* regulation functions that are dependent on the hydrogen partial pressure

190 ( $p_{H_2}$ ). This hybrid approach resulted by assuming a linearity between the couple NADH/NAD<sup>+</sup>

191 and the  $p_{H_2}$  following the work of (Mosey, 1983; Costello *et al.*, 1991). As discussed by (van

192 Lingen *et al.*, 2019), the production of acetate *via* the reaction R<sub>1</sub> is favoured at low

193 NADH/NAD<sup>+</sup> while the production of propionate *via* the reaction R<sub>2</sub> is favoured at high

194 NADH/NAD<sup>+</sup>. Accordingly, we represented the flux allocation parameters by the following

195 sigmoid functions:

196

$$197 \quad \lambda_1 = 1 - \frac{1}{1 + \exp(-p_5 \cdot (p_{H_2} + p_6))} \quad (7)$$

199 
$$\lambda_2 = \frac{p_7}{1 + \exp(-p_8 \cdot (p_{H_2} + p_9))}$$
 (8)

200 Our model then predicts that high levels of supplementation of *A. taxiformis* will result in high  
201 hydrogen levels that will favour propionate production ( $R_2$ ) over acetate production ( $R_1$ ). By  
202 this parameterization of the flux allocation parameters, our model accounts for the  
203 concomitant reduction of the acetate:propionate ratio that is observed when methane  
204 production is reduced.

### 206 2.3. Parameter estimation

207 We used the maximum likelihood estimator that minimizes the following objective function

209 
$$J(\mathbf{p}) = \sum_{k=1}^{n_y} \frac{n_{t,k}}{2} \ln \left[ \sum_{i=1}^{n_{t,k}} [y_k(t_{i_k}) - y_{m_k}(t_{i_k}, \mathbf{p})]^2 \right]$$
 (9)

210  
211 Where  $\mathbf{p}$  is the vector of parameters to be estimated,  $n_y$  is the number of measured variables,  
212  $n_{t,k}$  is the number of observation times of the variable  $k$ ,  $t_{i_k}$  is the  $i$ th measurement time for  
213 the variable  $y_k$ , and  $y_{m_k}$  is the value predicted by the model. The measured variables are the  
214 concentrations of acetate, butyrate, propionate,  $\text{NH}_3$ , and the moles of methane produced.

215 We used the IDEAS Matlab® toolbox (Muñoz-Tamayo *et al.*, 2009) (freely available at  
216 <http://genome.jouy.inra.fr/logiciels/IDEAS>) to generate the function files for solving the  
217 optimization problem locally. Then, we used the generated files by IDEAS to look for global  
218 optimal solutions using the Matlab optimization toolbox MEIGO (Egea *et al.*, 2014) that  
219 implements the enhanced scatter search method developed by (Egea *et al.*, 2010) for global  
220 optimization.

221  
222 We reduced substantially the number of parameters to be estimated by setting most of the  
223 model parameters to the values reported in the original model implementation and using the  
224 information obtained from the *in vitro* study (Chagas *et al.*, 2019). For example, the hydrolysis  
225 rate constant for NDF was obtained from (Chagas *et al.*, 2019) whereas the hydrolysis rate  
226 constants of NSC ( $k_{\text{hydr,nsc}}$ ) and proteins ( $k_{\text{hydr,pro}}$ ) were included in the parameter  
227 estimation problem. The kinetic rate constant for hydrogen utilization  $k_{m,H_2}$  was set 16  
228 mol/(mol h) using an average value of the values we obtained for the predominant archaea  
229 *Methanobrevibacter ruminantium* and *Methanobrevibacter smithii* (Muñoz-Tamayo *et al.*,  
230 2019) using a microbial yield factor of 0.006 mol biomass/mol  $\text{H}_2$  (Pavlostathis *et al.*, 1990).  
231 With this strategy, we penalize the goodness-of-fit of the model. But, on the other hand, we  
232 reduce practical identifiability problems typically found when calibrating biological kinetic-  
233 based models (Vanrolleghem *et al.*, 1995). The parameter vector for the estimation is then  $\mathbf{p}$ :  
234  $\{k_{\text{hydr,nsc}}, k_{\text{hydr,pro}}, k_{\text{br}}, p_1, p_2, \dots, p_9\}$ . The optimization was set in a multi-experiment fitting  
235 context that integrates the data of all treatments. To evaluate the model performance, we  
236 computed the determination coefficient ( $R^2$ ), the Lin's concordance correlation coefficient  
237 (CCC) (Lin, 1989), the Root mean squared error (RMSE) and the coefficient of variation of the  
238 RMSE ( $\text{CV}_{\text{RMSE}}$ ). We also performed residual analysis for bias assessment according to (St-  
239 Pierre, 2003).

## 240 3. Results

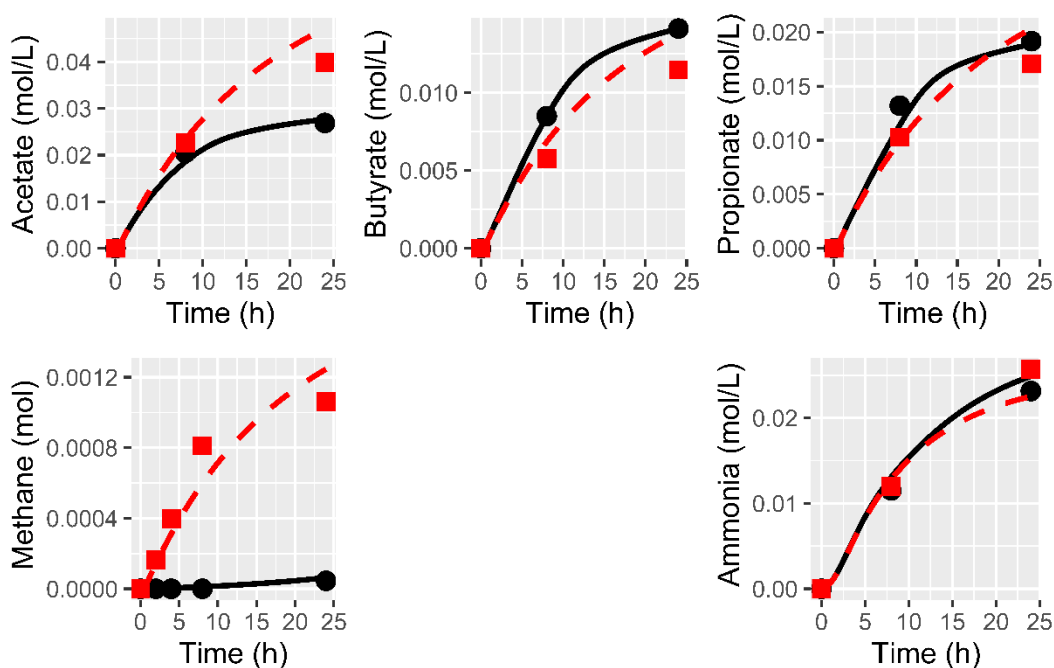
### 241 3.1. Dynamic prediction of rumen fermentation

242 The extended model developed in the present work to account for the impact of *A. taxiformis*  
243 on the rumen fermentation is freely available at <https://doi.org/10.5281/zenodo.4090332>  
244 with all the detailed information of the model and the experimental data used for model  
245 calibration. An open source version in the Scilab software (<https://www.scilab.org/>) was made  
246 available to facilitate reproductibility since Scilab files can be opened with a text editor. The  
247 software R (<https://www.r-project.org/>) was used to plot the figures.

248 Figure 2 shows the dynamic data of fermentation variables for the levels of *A. taxiformis* at  
249 0.06% and 0.5% compared against the model predicted variables. Figure 3 displays the  
250 comparison of all observations against model predictions. Figure 4 shows the residuals for all  
251 variables against centred predicted values.

252 To evaluate the performance of our model and its validation, external independent data is  
253 required. Due to data limitation, we did not perform such a validation. To provide indicators  
254 of our model, we calculated standard statistical indicators of model performance which are  
255 shown in Table 2. These statistic indicators are biased and thus should be looked with caution  
256 since they are calculated using the calibration data. Nevertheless, they provide an indication  
257 of the adequacy of the model structure to represent the fermentation dynamics. For methane,  
258 butyrate and NH<sub>3</sub> the mean and linear biases were not significant at the 5% significance level.  
259 Acetate and propionate exhibited significant linear bias. The liquid compounds have an  
260 average coefficient of variation of the RMSE (CV(RMSE)) of 11.25%. Methane had the higher  
261 CV(RMSE) (31%). The concordance correlation coefficients were higher than 0.93. Propionate  
262 had the lowest determination coefficient ( $R^2=0.82$ ) while methane and the other compounds  
263 had a  $R^2$  close to 0.9.

264



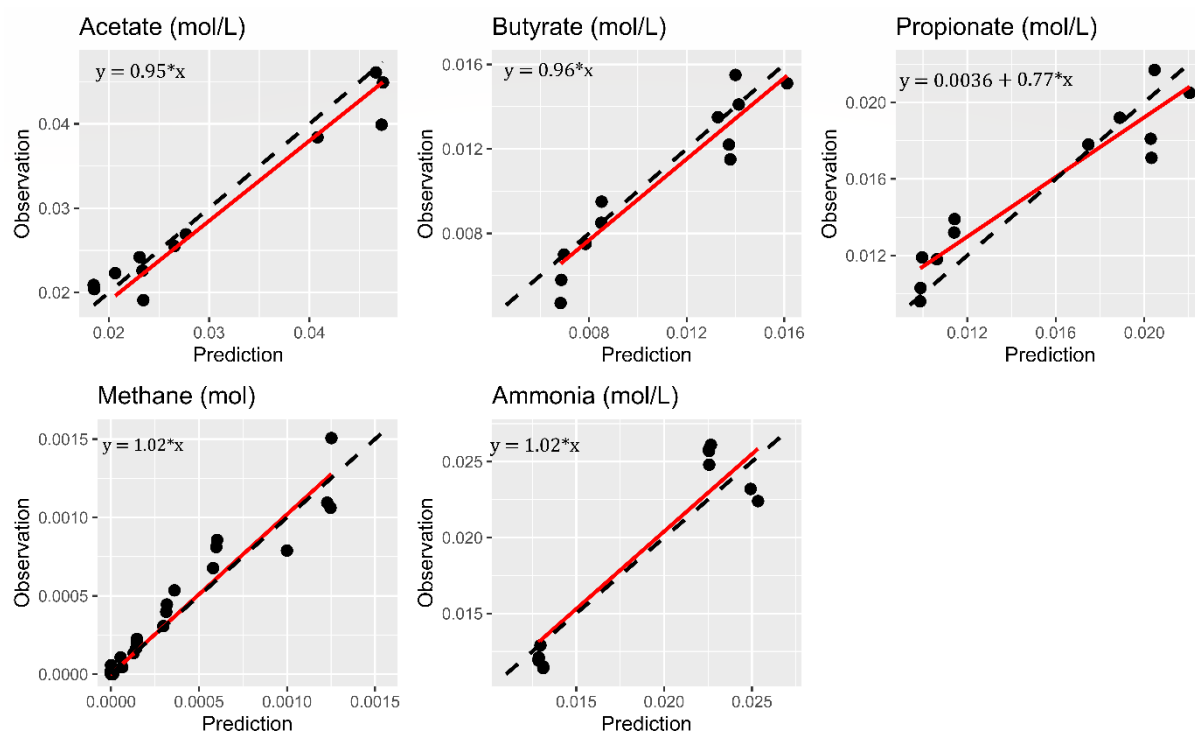
265

266

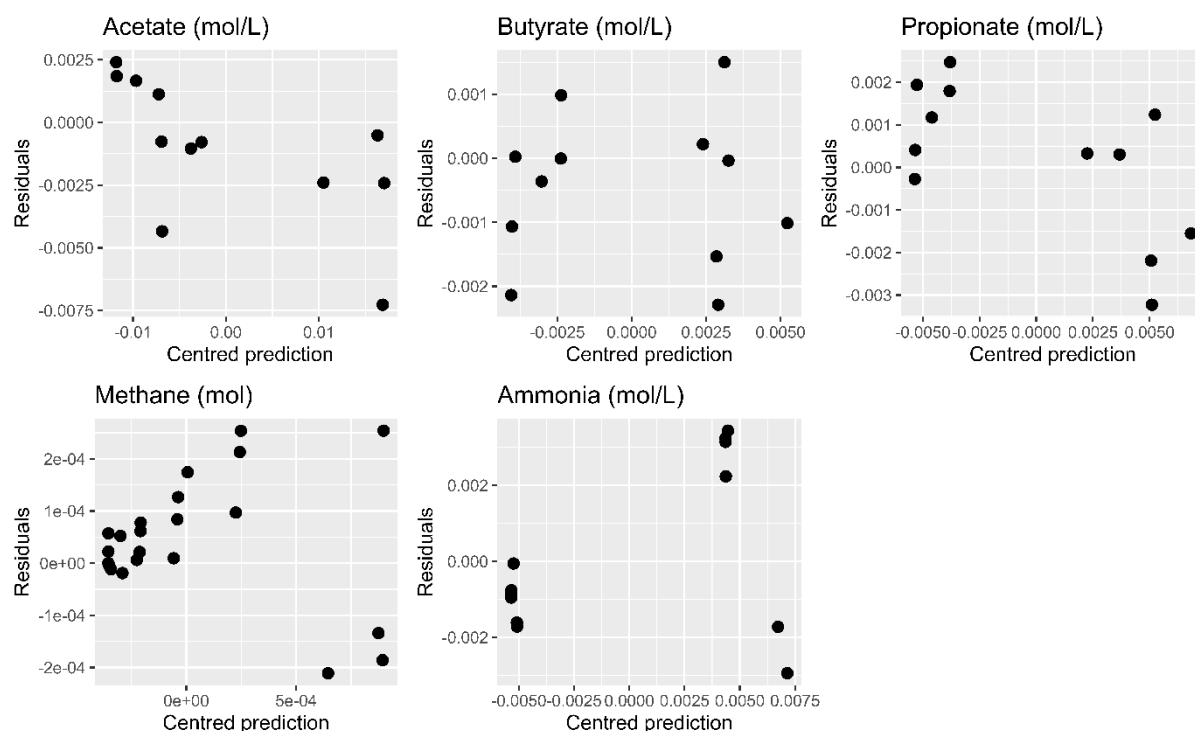
267 **Figure 2.** Example of model fitting. Experimental data of fermentation variables for the levels  
268 of *A. taxiformis* at 0.5% (●) and 0.06% (■) are compared against the model predicted responses  
269 in solid black lines (for 0.5% level) and in dashed red lines (for the 0.06% level).

270





271  
 272 **Figure 3.** Summary of the model performance calibration integrating data of all treatments.  
 273 Experimental data (●) are plotted against the model predicted variables. Solid lines are the  
 274 linear fitted curve. Dashed lines are the isoclines. Only the intercept of the curve of propionate  
 275 was different from zero at 5% significance level.  
 276



277  
 278 **Figure 4.** Residuals values of observed variables against centred predicted variables ( $n_{CH_4}$   
 279  $=24$ ,  $n_{NH_3} = n_{ac} = n_{bu} = n_{pr} = 12$ ).  
 280  
 281  
 282

283 **Table 2.** Statistical indicators of model performance.

	Acetate	Butyrate	Propionate	Methane	NH <sub>3</sub>
R <sup>2</sup>	0.91	0.88	0.82	0.92	0.89
RMSE <sup>a</sup>	0.0029	0.0012	0.0017	1.21x10 <sup>-4</sup>	0.002
100×CV <sub>RMSE</sub> <sup>b</sup>	10	12	11	31	12
CCC <sup>c</sup>	0.96	0.94	0.93	0.96	0.93

Residual analysis					
$residual = \alpha + \beta \cdot (predicted - mean\ predicted\ value)$					
	Acetate	Butyrate	Propionate	Methane	NH <sub>3</sub>
$\alpha$ ( $p$ -value)	-0.0010 ( $p=0.14$ )	-0.00047 ( $p=0.21$ )	0.00019 ( $p=0.63$ )	4.0e-05 ( $p=0.12$ )	0.00012 ( $p=0.86$ )
$\beta$ ( $p$ -value)	-0.15 ( $p=0.024$ )	0.0028 ( $p=0.98$ )	-0.22 ( $p=0.024$ )	-0.031 ( $p=0.60$ )	0.15 ( $p=0.23$ )

284 <sup>a</sup> Root mean squared error (RMSE).

285 <sup>b</sup> Coefficient of variation of the RMSE (CV(RMSE)).

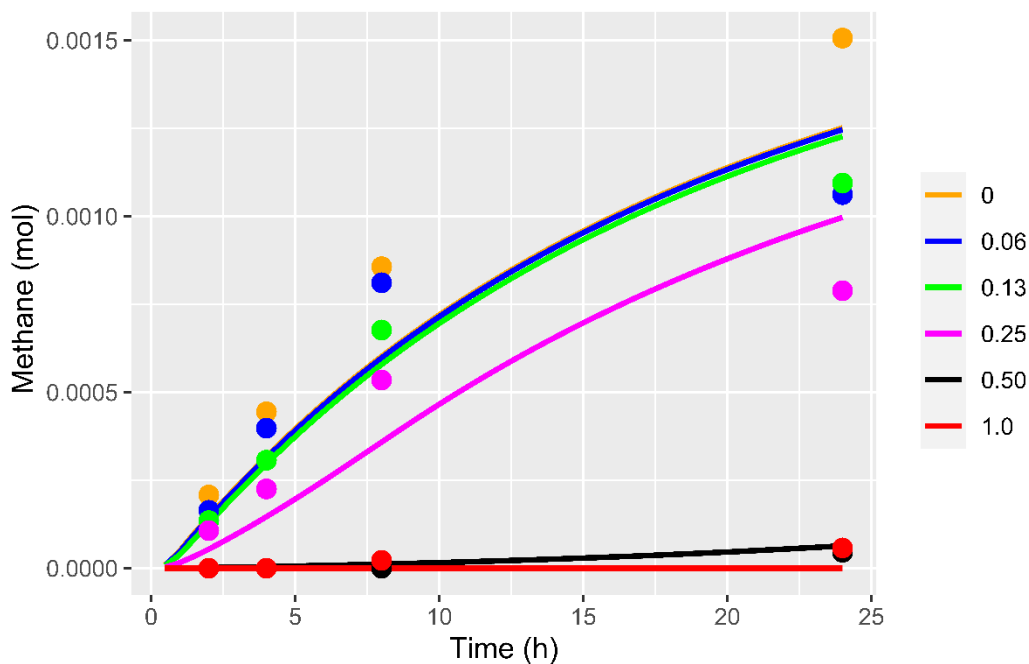
286 <sup>c</sup> Concordance correlation coefficient (CCC)

287

288 Figure 5 compares specifically the experimental data of methane against the model

289 predictions for all levels of *A. taxiformis*.

290



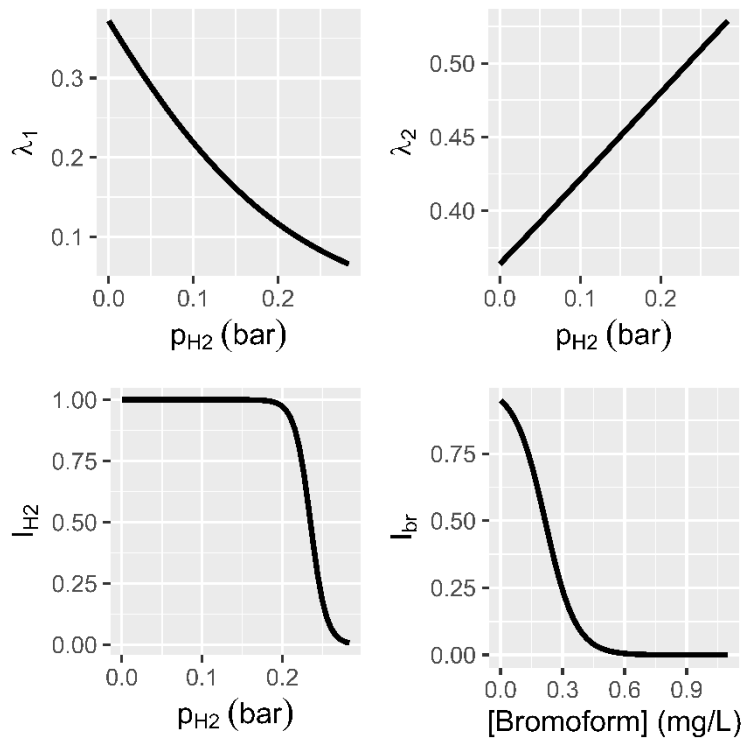
291

292 **Figure 5.** Experimental observations of methane (circles) in the headspace of the incubation  
 293 system are compared against the model predicted values (solid lines). Increase of the dose of  
 294 *A. taxiformis* results in a decrease of methane production.

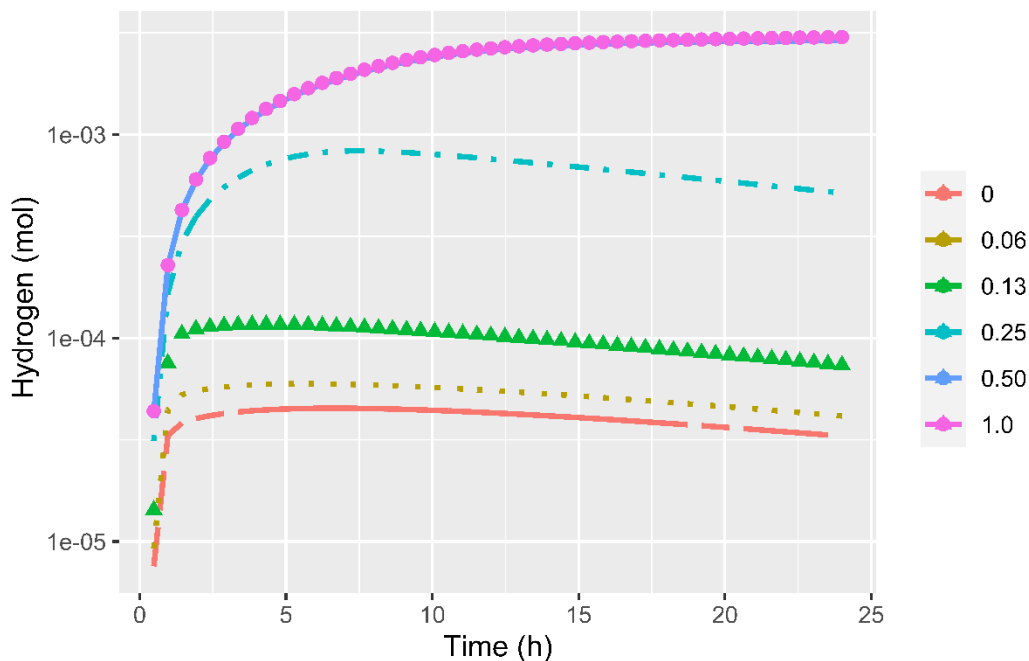
295

### 296 **3.2. Prediction of the factors representing the impact of *A.*** 297 ***taxiformis* on rumen fermentation**

298 Figure 6 plots the factors that represent the effect of *A. taxiformis* on rumen fermentation.  
 299 Direct inhibition of the methanogenesis due to the anti-methanogenic action of bromoform  
 300 is represented by the factor  $I_{br}$ . Methanogenesis inhibition results in hydrogen accumulation  
 301 impacting the flux allocation of sugars utilization.



302  
303 **Figure 6.** In our model, the effect of *A. taxiformis* on rumen fermentation is represented by a  
304 direct inhibitory effect of bromoform ( $I_{br}$ ) on the methanogens growth rate. Methanogenesis  
305 inhibition results in hydrogen accumulation. Hydrogen control impacts sugar utilization by  
306 inhibiting the rate of sugar utilization (factor  $I_{H_2}$ ) and by regulating the flux allocation  
307 parameters ( $\lambda_1, \lambda_2$ ) towards VFA production.  
308 Figure 7 displays the simulated dynamics of hydrogen in the headspace for all the  
309 supplementation levels of *A. taxiformis*. For supplementation levels higher than 0.25%, the  
310 methanogenesis inhibition resulted in a substantial hydrogen accumulation.



311  
312 **Figure 7.** Predicted dynamics of hydrogen in the headspace for levels of *A. taxiformis*. Increase  
313 of the dose of *A. taxiformis* results in an increase of hydrogen in the incubation system.

## 314 4. Discussion

315 The goal of this work was to model the impact of *A. taxiformis* supplementation on the rumen  
316 microbial fermentation and methane production under *in vitro* conditions using experimental  
317 data from (Chagas *et al.*, 2019). Overall, our model was able to capture the dynamics of VFA,  
318 ammonia and methane production for different levels of *A. taxiformis* indicating the potential  
319 of the model structure towards the development of predictive models for assessing methane  
320 mitigation strategies in ruminants. With the exception of propionate, the slope of observed vs  
321 predicted variables is very close to one. Model limitations will be discussed further. We  
322 modelled the effect of *A. taxiformis* on rumen fermentation by two mechanisms. The first  
323 mechanism is associated to the direct inhibition of the methanogens growth rate by the anti-  
324 methanogenic compounds of *A. taxiformis* documented in different studies (Kinley *et al.*,  
325 2016; Machado *et al.*, 2016a; Roque *et al.*, 2019). In our model, we ascribed the inhibitory  
326 effect of *A. taxiformis* only to the concentration of bromoform. The first-order kinetic rate for  
327 bromoform consumption and the inhibition factor ( $I_{br}$ ) (Fig. 6) allowed our model to account  
328 for the observed dynamic decline in methanogenesis inhibition (Kinley *et al.*, 2016). It should  
329 be noted that although bromoform is the most abundant anti-methanogenic compound in *A.*  
330 *taxiformis*, the anti-methanogenic capacity of *A. taxiformis* is the result of the synergetic  
331 action of all halogenated products present in the macroalgae (Machado *et al.*, 2016b) .  
332 Accordingly, it will be useful to include further in our model other secondary compounds such  
333 as dibromochloromethane. To enhance our model, it will be central to perform new  
334 experiments to characterize the dynamics of anti-methanogenic compounds. This aspect is of  
335 great relevance to allow the model to be adapted to different applications of seaweed  
336 supplementation since it is known that the composition of halogenic compounds can vary with  
337 respect to the season, harvesting and drying methods.  
338 The second mechanism that accounts for the impact of *A. taxiformis* on the fermentation is  
339 hydrogen control, which it is discussed below.

340

### 341 4.1. Methane inhibition and hydrogen control

342 The anti-methanogenic capacity of *A. taxiformis* is dose-dependent. The experimental study  
343 of (Chagas *et al.*, 2019) showed that methane production was inhibited almost completely by  
344 *A. taxiformis* at a level of 0.5%. Our model predictions aligned with the experimental  
345 observations (Fig. 5). The anti-methanogenic capacity of the macroalgae leads to hydrogen  
346 accumulation (Kinley *et al.*, 2020; Roque *et al.*, 2020) as predicted by our model in Fig. 7. The  
347 level of hydrogen increases as the dose of *A. taxiformis* increases. The predicted values of  
348 hydrogen levels in the headspace for low doses of *A. taxiformis* showing in Figure 7 are in  
349 agreement with *in vitro* reported values (Serment *et al.*, 2016). The level of hydrogen can  
350 impact electron-mediating cofactors such as nicotinamide adenine dinucleotide (NAD) which  
351 are important drivers of anaerobic metabolism *via* the transfer of electrons in metabolic redox  
352 reactions (Hoelzle *et al.*, 2014). van Lingen *et al.*, 2019 extended the rumen model developed  
353 by (Dijkstra *et al.*, 1992) to incorporate the regulation of NADH/NAD<sup>+</sup> on the fermentation.

354

355 In our model, the regulation of NADH/NAD<sup>+</sup> was incorporated *via* the control of hydrogen  
356 partial pressure assuming a linearity between the couple NADH/NAD<sup>+</sup> and the  $p_{\text{H}_2}$  and  
357 following the model structure proposed by (Mosey, 1983) with a different parameterisation  
358 for the functions describing the effect of  $p_{\text{H}_2}$  on the rate of glucose utilization and on the flux  
359 allocation. The linearity assumption between NADH/NAD<sup>+</sup> and the  $p_{\text{H}_2}$  might not be fulfilled  
360 for all values of  $p_{\text{H}_2}$  (De Kok et al., 2013). In the experimental conditions used in the  
361 experiment here analysed (Chagas et al., 2019) and under rumen physiological conditions, the  
362 linearity between NADH/NAD<sup>+</sup> might be valid.

363 With regard to the hydrogen control on glucose utilization, our model predicts that the  
364 inhibition is effective at  $p_{\text{H}_2}$  higher than 0.2 bar (factor  $I_{\text{H}_2}$  in Fig. 6). In our model, the  
365 incorporation of the inhibitory effect of hydrogen was motivated to account for the decrease  
366 of the total production of VFA at high levels of supplementation of *A. taxiformis* observed by  
367 (Chagas *et al.*, 2019). Such a decrease of VFA production is dose-dependent as observed in *in*  
368 *vitro* studies (Kinley *et al.*, 2016; Machado *et al.*, 2016a). *In vivo*, while insignificant changes in  
369 total VFA concentration between a control diet and diets with *A. taxiformis* supplementation  
370 were observed in Brangus steers (Kinley *et al.*, 2020), inclusions of *A. taxiformis* resulted in a  
371 decrease in total VFA ruminal concentration in sheep compared with control diet (Li *et al.*,  
372 2016). Accordingly, additional studies with simultaneous measurements of VFA and hydrogen  
373 are needed to validate the relevance of the inhibitory term  $I_{\text{H}_2}$  of our model both under *in*  
374 *vitro* and *in vivo* conditions.

375 In addition to the impact of *A. taxiformis* supplementation on methane reduction, it is  
376 important to look at the effects on animal productivity. *A. taxiformis* impacts the production  
377 of VFAs, which are energy sources for the animal. Accordingly, changes in VFA production  
378 might result in changes on productivity and feed efficiency. Optimal feeding strategies should  
379 thus be designed to attain a trade-off between low methane emissions and high productivity  
380 and animal health. Studies showing the effect of *A. taxiformis* supplementation on live weight  
381 (Li *et al.*, 2016), average daily weight gain and feed conversion efficiency (Kinley *et al.*, 2020;  
382 Roque *et al.*, 2020) are still scarce to provide a large data base for concluding on the impact  
383 of *A. taxiformis* on animal productivity and feed efficiency. However, the studies of (Kinley *et*  
384 *al.*, 2020; Roque *et al.*, 2020) suggest that feed conversion efficiency tend to increase  
385 concomitantly with the reduction of methane production induced by an adequate  
386 supplementation of *A. taxiformis*, supporting the theory of redirection of energy otherwise  
387 lost as methane (Kinley *et al.*, 2020). An opportunity to enhance the action of *A. taxiformis*  
388 might be the implementation of a feeding strategy integrating macroalgae supplementation  
389 with an adequate additive allowing to redirect metabolic hydrogen towards nutritional  
390 fermentation products beneficial to the animal. Such a strategy will fulfil the objectives of  
391 reducing methane emissions while increasing animal productivity (Ungerfeld, 2020).

392  
393 With regard to the fermentation pattern, when the hydrogen level increases the hydrogen  
394 control operates by increasing the flux of carbon towards propionate ( $\lambda_2$ ) while the flux  
395 towards the reaction that produces only acetate ( $\lambda_1$ ) decreases (Fig. 6). Incorporating  
396 hydrogen control on the fermentation pattern in our model enabled us to predict the decrease  
397 of the acetate to propionate ratio observed at levels of *A. taxiformis* supplementation leading  
398 to substantial methane reduction both *in vitro* (Machado *et al.*, 2016a; Chagas *et al.*, 2019)  
399 and *in vivo* (Kinley *et al.*, 2020). Our model is also consistent with *in vitro* (Kinley *et al.*, 2016;

400 Machado *et al.*, 2016a) and *in vivo* (Stefenoni *et al.*, 2021) studies showing the increase of  
401 butyrate level when the inclusion of *A. taxiformis* increases.

## 402 **4.2. Model limitations and perspectives**

403 In our model, the quantification of the impact of *A. taxiformis* was ascribed by the action of  
404 bromoform on the methanogens growth rate and by the action of  $p_{H_2}$  on the fermentation  
405 pattern. However, in the experimental study of (Chagas *et al.*, 2019), nor bromoform nor  
406  $p_{H_2}$  were measured. From our bibliography search, we did not find studies reporting dynamic  
407 measurements of bromoform. Although we did not perform an identifiability analysis, we might  
408 expect that the lack of bromoform and hydrogen data in our work might result in structural  
409 identifiability (Muñoz-Tamayo *et al.*, 2018) and model distinguishability problems (Walter and  
410 Pronzato, 1996). We will then require external data to validate our model. Experiments to be  
411 done within the MASTER project (<https://www.master-h2020.eu/contact.html>) will fill this  
412 gap and provide data for challenging and improving our model.

413 Our model aligns with the efforts of enhancing the dynamic prediction of ruminal metabolism  
414 *via* the incorporation of thermodynamics and regulation factors (Offner and Sauvant, 2006;  
415 Ghimire *et al.*, 2014; van Lingen *et al.*, 2019). While our work focused only on hydrogen control  
416 on sugars metabolism, future work is needed to incorporate the impact of *A. taxiformis*  
417 supplementation on amino acids fermentation. The study of (Chagas *et al.*, 2019) showed a  
418 decrease of branched-chain volatile fatty acids (BCVFA ) with increased supplementation of *A.*  
419 *taxiformis*. Such a decrease of BCVFA might have a negative influence on microbial activity.

420 We modelled the regulation of sugars metabolism by hydrogen control following a grey-box  
421 modelling approach where the regulation factors were assigned to sigmoid functions without  
422 an explicit mechanistic interpretation. However, to enhance the understanding of rumen  
423 fermentation, it will be useful to pursue an approach incorporating the role of internal  
424 electron mediating cofactors on the direction of electrons towards hydrogen or VFA (Hoelzle  
425 *et al.*, 2014; Ungerfeld, 2020). Recent progress in this area (van Lingen *et al.*, 2019) opens a  
426 direction for improving the prediction of rumen models.

427 The ultimate goal of this work is to pursue a model extension to account for *in vivo* conditions.  
428 In this endeavour, experimental data in semi-continuous devices such as the Rusitec (Roque  
429 *et al.*, 2019a) will be instrumental for model improvement. *In vivo*, in addition to the impact  
430 on fermentation, *A. taxiformis* can induce changes in rumen mucosa (Li *et al.*, 2016). These  
431 mucosa changes might translate in changes on the rate of absorption of ruminal VFA. This  
432 effect on the rate of VFA absorption should be quantified and incorporated into an extended  
433 model. In our model, the pH was set constant. However, pH exhibits a dynamic behaviour that  
434 can impact the activity of the rumen microbiota. The impact of the pH on the rumen microbial  
435 groups should be then considered in a future version of the model, integrating the mechanistic  
436 calculation of pH elaborated in our previous model (Muñoz-Tamayo *et al.*, 2016).

437

438

439

440 Finally, although our model developments focused on the impact of *A. taxiformis* on rumen  
441 fermentation and methane production, we think our model structure has the potential to be  
442 applied to other additives such as 3-nitrooxypropanol (Hristov *et al.*, 2015; Duin *et al.*, 2016)  
443 whose action is specifically directed to inhibit methanogenic archaea, as the halogenated  
444 compounds of *A. taxiformis*. We expect these model developments can be useful to help the  
445 design of sustainable nutritional strategies promoting healthy rumen function and low  
446 environmental footprint.

## 447 **5. Conclusions**

448 We have developed a rumen fermentation model that accounts for the impact of *A. taxiformis*  
449 supply on *in vitro* rumen fermentation and methane production. Our model was effective in  
450 representing the dynamics of VFA, ammonia and methane for six supplementation levels of  
451 *A. taxiformis*, providing a promising prediction tool for assessing the impact of additives such  
452 as seaweeds on rumen microbial fermentation and methane production *in vitro*.

## 453 **6. Declarations**

454 **Ethics approval:** Not applicable

### 455 **Availability of data and material**

456 The datasets and codes used in this study are available at  
457 <https://doi.org/10.5281/zenodo.4090332>

### 458 **Funding**

459 Authors acknowledge funding from the RumenPredict project funded by the Horizon2020  
460 Research & Innovation Programme under grant agreement No 696356. Rafael Muñoz-Tamayo  
461 acknowledges funding from the MASTER project, an Innovation Action funded by the  
462 European Union's Horizon 2020 research and innovation programme under grant agreement  
463 No 818368.

### 464 **Acknowledgements**

465 Authors thank Henk van Lingen (Wageningen University, The Netherlands), Alberto Atzori  
466 (University of Sassari, Italy) and two anonymous reviewers appointed by Luis Tedeschi (Texas  
467 A&M University, USA) for the evaluation of this manuscript by PCI Animal Science  
468 (<https://animsci.peercommunityin.org/>). Their reviews have greatly improved this paper.

### 469 **Authors' contributions**

470 JCC, MH and SJC produced the experimental data of the study. RMT developed the  
471 mathematical model and drafted the article. All authors contributed to the analysis and  
472 interpretation of the results. All authors read and approved the final manuscript.

473

## 474 **Conflict of interest disclosure**

475 The authors of this article declare that they have no financial conflict of interest with the  
476 content of this article. Rafael Muñoz-Tamayo is editor of PCI Animal Science.

## 477 **7. References**

- 478 Beauchemin, K.A., Ungerfeld, E.M., Eckard, R.J., and Wang, M. (2020) Review: Fifty years of  
479 research on rumen methanogenesis: Lessons learned and future challenges for  
480 mitigation. *Animal* **14**(S1): S2–S16.
- 481 Chagas, J.C., Ramin, M., and Krizsan, S.J. (2019) In vitro evaluation of different dietary  
482 methane mitigation strategies. *Animals* **9**: 1120.
- 483 Chalupa, W. (1977) Manipulating Rumen Fermentation. *J Anim Sci* **46**: 585–599.
- 484 Costello, D.J., Greenfield, P.F., and Lee, P.L. (1991) Dynamic Modeling of a Single-Stage High-  
485 Rate Anaerobic Reactor .1. Model Derivation. *Water Res* **25**: 847–858.
- 486 Czerkawski, J.W. and Breckenridge, G. (1975) New inhibitors of methane production by  
487 rumen micro-organisms. Development and testing of inhibitors in vitro. *Br J Nutr* **34**:  
488 429–446.
- 489 Denman, S.E., Tomkins, N.W., and McSweeney, C.S. (2007) Quantitation and diversity  
490 analysis of ruminal methanogenic populations in response to the antimethanogenic  
491 compound bromochloromethane. *FEMS Microbiol Ecol* **62**: 313–322.
- 492 Dijkstra, J., Neal, H.D., Beever, D.E., and France, J. (1992) Simulation of nutrient digestion,  
493 absorption and outflow in the rumen: model description. *J Nutr* **122**: 2239–2256.
- 494 Dubois, B., Tomkins, N.W., D. Kinley, R., Bai, M., Seymour, S., A. Paul, N., and Nys, R. de  
495 (2013) Effect of Tropical Algae as Additives on Rumen *in Vitro* Gas Production and  
496 Fermentation Characteristics. *Am J Plant Sci* **4**: 34–43.
- 497 Duin, E.C., Wagner, T., Shima, S., Prakash, D., Cronin, B., Yáñez-Ruiz, D.R., et al. (2016) Mode  
498 of action uncovered for the specific reduction of methane emissions from ruminants by  
499 the small molecule 3-nitrooxypropanol. *Proc Natl Acad Sci U S A* **113**: 6172–6177.
- 500 Egea, J.A., Henriques, D., Cokelaer, T., Villaverde, A.F., MacNamara, A., Danciu, D.P., et al.  
501 (2014) MEIGO: An open-source software suite based on metaheuristics for global  
502 optimization in systems biology and bioinformatics. *BMC Bioinformatics* **15**: 136.
- 503 Egea, J.A., Martí, R., and Banga, J.R. (2010) An evolutionary method for complex-process  
504 optimization. *Comput Oper Res* **37**: 315–324.
- 505 Ellis, J.L., Dijkstra, J., France, J., Parsons, A.J., Edwards, G.R., Rasmussen, S., et al. (2012)  
506 Effect of high-sugar grasses on methane emissions simulated using a dynamic model. *J*  
507 *Dairy Sci* **95**: 272–285.
- 508 Evans, F.D. and Critchley, A.T. (2014) Seaweeds for animal production use. *J Appl Phycol* **26**:



- 509 891–899.
- 510 Ghimire, S., Gregorini, P., and Hanigan, M.D. (2014) Evaluation of predictions of volatile fatty  
511 acid production rates by the Molly cow model. *J Dairy Sci* **97**: 354–362.
- 512 Hoelzle, R.D., Viridis, B., and Batstone, D.J. (2014) Regulation mechanisms in mixed and pure  
513 culture microbial fermentation. *Biotechnol Bioeng* **111**: 2139–2154.
- 514 Hristov, A.N., Oh, J., Giallongo, F., Frederick, T.W., Harper, M.T., Weeks, H.L., et al. (2015) An  
515 inhibitor persistently decreased enteric methane emission from dairy cows with no  
516 negative effect on milk production. *Proc Natl Acad Sci U S A* **112**: 10663–10668.
- 517 Huws, S.A., Creevey, C.J., Oyama, L.B., Mizrahi, I., Denman, S.E., Popova, M., et al. (2018)  
518 Addressing global ruminant agricultural challenges through understanding the rumen  
519 microbiome: past, present, and future. *Front Microbiol* **9**: 2161.
- 520 Janssen, P.H. (2010) Influence of hydrogen on rumen methane formation and fermentation  
521 balances through microbial growth kinetics and fermentation thermodynamics. *Anim*  
522 *Feed Sci Technol* **160**: 1–22.
- 523 Kettle, H., Holtrop, G., Louis, P., and Flint, H.J. (2018) microPop: Modelling microbial  
524 populations and communities in R. *Methods Ecol Evol* **9**: 399–409.
- 525 Kinley, R.D., Martinez-Fernandez, G., Matthews, M.K., de Nys, R., Magnusson, M., and  
526 Tomkins, N.W. (2020) Mitigating the carbon footprint and improving productivity of  
527 ruminant livestock agriculture using a red seaweed. *J Clean Prod* **259**: 120836.
- 528 Kinley, R.D., De Nys, R., Vucko, M.J., MacHado, L., and Tomkins, N.W. (2016) The red  
529 macroalgae *Asparagopsis taxiformis* is a potent natural antimethanogenic that reduces  
530 methane production during in vitro fermentation with rumen fluid. *Anim Prod Sci* **56**:  
531 282–289.
- 532 Li, X., Norman, H.C., Kinley, R.D., Laurence, M., Wilmot, M., Bender, H., et al. (2016)  
533 *Asparagopsis taxiformis* decreases enteric methane production from sheep. *Anim Prod*  
534 *Sci* **58**: 681–688.
- 535 Lin, L.I. (1989) A concordance correlation-coefficient to evaluate reproducibility. *Biometrics*  
536 **45**: 255–268.
- 537 van Lingen, H.J., Fadel, J.G., Moraes, L.E., Bannink, A., and Dijkstra, J. (2019) Bayesian  
538 mechanistic modeling of thermodynamically controlled volatile fatty acid, hydrogen and  
539 methane production in the bovine rumen. *J Theor Biol* **480**: 150–165.
- 540 Machado, L., Magnusson, M., Paul, N.A., Kinley, R., de Nys, R., and Tomkins, N. (2016a) Dose-  
541 response effects of *Asparagopsis taxiformis* and *Oedogonium* sp. on in vitro  
542 fermentation and methane production. *J Appl Phycol* **28**: 1443–1452.
- 543 Machado, L., Magnusson, M., Paul, N.A., Kinley, R., de Nys, R., and Tomkins, N. (2016b)  
544 Identification of bioactives from the red seaweed *Asparagopsis taxiformis* that promote  
545 antimethanogenic activity in vitro. *J Appl Phycol* **28**: 3117–3126.

- 546 Machado, L., Magnusson, M., Paul, N.A., De Nys, R., and Tomkins, N. (2014) Effects of marine  
547 and freshwater macroalgae on in vitro total gas and methane production. *PLoS One* **9**:  
548 e85289.
- 549 Machado, L., Tomkins, N., Magnusson, M., Midgley, D.J., de Nys, R., and Rosewarne, C.P.  
550 (2018) In Vitro Response of Rumen Microbiota to the Antimethanogenic Red Macroalga  
551 *Asparagopsis taxiformis*. *Microb Ecol* **75**: 811–818.
- 552 Maia, M.R.G., Fonseca, A.J.M., Oliveira, H.M., Mendonça, C., and Cabrita, A.R.J. (2016) The  
553 potential role of seaweeds in the natural manipulation of rumen fermentation and  
554 methane production. *Sci Rep* **6**: 32321.
- 555 Makkar, H.P.S., Tran, G., Heuzé, V., Giger-Reverdin, S., Lessire, M., Lebas, F., and Ankers, P.  
556 (2016) Seaweeds for livestock diets: A review. *Anim Feed Sci Technol* **212**: 1–17.
- 557 Mosey, F.E. (1983) Mathematical-Modeling of the Anaerobic-Digestion Process - Regulatory  
558 Mechanisms for the Formation of Short-Chain Volatile Acids from Glucose. *Water Sci*  
559 *Technol* **15**: 209–232.
- 560 Muñoz-Tamayo, R., Giger-Reverdin, S., and Sauvant, D. (2016) Mechanistic modelling of in  
561 vitro fermentation and methane production by rumen microbiota. *Anim Feed Sci*  
562 *Technol* **220**: 1–21.
- 563 Muñoz-Tamayo, R., Laroche, B., Leclerc, M., and Walter, E. (2009) IDEAS: A parameter  
564 identification toolbox with symbolic analysis of uncertainty and its application to  
565 biological modelling. In, *IFAC Proceedings Volumes.*, pp. 1271–1276.
- 566 Muñoz-Tamayo, R., Popova, M., Tillier, M., Morgavi, D.P., Morel, J.P., Fonty, G., and Morel-  
567 Desrosiers, N. (2019) Hydrogenotrophic methanogens of the mammalian gut:  
568 Functionally similar, thermodynamically different—A modelling approach. *PLoS One* **14**:  
569 e0226243.
- 570 Muñoz-Tamayo, R., Puillet, L., Daniel, J.B., Sauvant, D., Martin, O., Taghipoor, M., and Blavy,  
571 P. (2018) Review: To be or not to be an identifiable model. Is this a relevant question in  
572 animal science modelling? *Animal* **12**: 701–712.
- 573 Offner, A. and Sauvant, D. (2006) Thermodynamic modeling of ruminal fermentations. **55**:  
574 343–365.
- 575 Paul, N.A., De Nys, R., and Steinberg, P.D. (2006) Chemical defence against bacteria in the  
576 red alga *Asparagopsis armata*: Linking structure with function. *Mar Ecol Prog Ser* **306**:  
577 87–101.
- 578 Pavlostathis, S.G., Miller, T.L., and Wolin, M.J. (1990) Cellulose Fermentation by Continuous  
579 Cultures of *Ruminococcus-Albus* and *Methanobrevibacter-Smithii*. *Appl Microbiol*  
580 *Biotechnol* **33**: 109–116.
- 581 Puhakka, L., Jaakkola, S., Simpura, I., Kokkonen, T., and Vanhatalo, A. (2016) Effects of  
582 replacing rapeseed meal with fava bean at 2 concentrate crude protein levels on feed

- 583 intake, nutrient digestion, and milk production in cows fed grass silage–based diets. *J*  
584 *Dairy Sci* **99**: 7993–8006.
- 585 Ramin, M. and Huhtanen, P. (2012) Development of an in vitro method for determination of  
586 methane production kinetics using a fully automated in vitro gas system-A modelling  
587 approach. *Anim Feed Sci Technol* **174**: 190–200.
- 588 Roque, B.M., Brooke, C.G., Ladau, J., Polley, T., Marsh, L.J., Najafi, N., et al. (2019) Effect of  
589 the macroalgae *Asparagopsis taxiformis* on methane production and rumen  
590 microbiome assemblage. *Anim Microbiome* **1:3**:
- 591 Roque, B.M., Salwen, J.K., Kinley, R., and Kebreab, E. (2019) Inclusion of *Asparagopsis armata*  
592 in lactating dairy cows' diet reduces enteric methane emission by over 50 percent. *J*  
593 *Clean Prod* **234**: 132–138.
- 594 Roque, B.M., Venegas, M., Kinley, R., DeNys, R., Neoh, T.L., Duarte, T.L., et al. (2020) Red  
595 seaweed (*Asparagopsis taxiformis*) supplementation reduces enteric methane by over  
596 80 percent in beef steers. *bioRxiv*.
- 597 St-Pierre, N.R. (2003) Reassessment of Biases in Predicted Nitrogen Flows to the Duodenum  
598 by NRC 2001. *J Dairy Sci* **86**: 344–350.
- 599 Stefenoni, H.A., Räisänen, S.E., Cueva, S.F., Wasson, D.E., Lage, C.F.A., Melgar, A., et al.  
600 (2021) Effects of the macroalga *Asparagopsis taxiformis* and oregano leaves on  
601 methane emission, rumen fermentation, and lactational performance of dairy cows. *J*  
602 *Dairy Sci*.
- 603 Ungerfeld, E.M. (2020) Metabolic Hydrogen Flows in Rumen Fermentation: Principles and  
604 Possibilities of Interventions. *Front Microbiol* **11**: 589.
- 605 Vanrolleghem, P.A., Vandaele, M., and Dochain, D. (1995) Practical identifiability of a  
606 biokinetic model of activated-sludge respiration. *Water Res* **29**: 2561–2570.
- 607 Walter, E. and Pronzato, L. (1996) On the identifiability and distinguishability of nonlinear  
608 parametric models. *Math Comput Simul* **42**: 125–134.
- 609 Wang, Y., Xu, Z., Bach, S.J., and McAllister, T.A. (2008) Effects of phlorotannins from  
610 *Ascophyllum nodosum* (brown seaweed) on in vitro ruminal digestion of mixed forage  
611 or barley grain. *Anim Feed Sci Technol* **145**: 375–395.
- 612 Wood, J.M., Kennedy, F.S., and Wolfe, R.S. (1968) The Reaction of Multihalogenated  
613 Hydrocarbons with Free and Bound Reduced Vitamin B12. *Biochemistry* **7**: 1707–1713.
- 614